^{9}Be + ^{120}Sn scattering at near-barrier energies within a four-body model

A. Arazi,[1,2,*] J. Casal,[3,4,†] M. Rodríguez-Gallardo,[3] J. M. Arias,[3] R. Lichtenthäler Filho,[5] D. Abriola,[1] O. A. Capurro,[1] M. A. Cardona,[1,2] P. F. F. Carnelli,[1,2] E. de Barbará,[1] J. Fernández Niello,[1,2] J. M. Figueira,[1,2] L. Fimiani,[1] D. Hojman,[1,2] G. V. Martí,[1] D. Martínez Heimman,[1,2] and A. J. Pacheco[1,2]

[1]*Laboratorio TANDAR, Comisión Nacional de Energía Atómica, Av. Gral. Paz 1499, BKNA1650 San Martín, Argentina*

[2]*Consejo Nacional de Investigaciones Científicas y Técnicas, Av. Rivadavia 1917, C1033AAJ Buenos Aires, Argentina*

[3]*Departamento de Física Atómica, Molecular y Nuclear, Facultad de Física, Universidad de Sevilla, Apartado 1065, E-41080 Sevilla, Spain*

[4]*European Centre for Theoretical Studies in Nuclear Physics and Related Areas (ECT*) and Fondazione Bruno Kessler, Villa Tambosi, Strada delle Tabarelle 286, I-38123 Villazzano (TN), Italy*

[5]*Departamento de Física Nuclear, Instituto de Física da Universidade de São Paulo, 05508-090 São Paulo, SP, Brazil*

(Received 29 July 2017; revised manuscript received 29 December 2017; published 18 April 2018)

Cross sections for elastic and inelastic scattering of the weakly bound ^{9}Be nucleus on a ^{120}Sn target have been measured at seven bombarding energies around and above the Coulomb barrier. The elastic angular distributions are analyzed with a four-body continuum-discretized coupled-channels (CDCC) calculation, which considers ^{9}Be as a three-body projectile ($\alpha + \alpha + n$). An optical model analysis using the São Paulo potential is also shown for comparison. The CDCC analysis shows that the coupling to the continuum part of the spectrum is important for the agreement with experimental data even at energies around the Coulomb barrier, suggesting that breakup is an important process at low energies. At the highest incident energies, two inelastic peaks are observed at 1.19(5) and 2.41(5) MeV. Coupled-channels (CC) calculations using a rotational model confirm that the first inelastic peak corresponds to the excitation of the 2^{+}_{1} state in ^{120}Sn, while the second one likely corresponds to the excitation of the 3^{-}_{1} state.

DOI: 10.1103/PhysRevC.97.044609

I. INTRODUCTION

Weakly bound and exotic nuclei have been intensively studied due to their role in astrophysics [1] and as a test for theoretical models capable of describing their singular structure and complex reaction mechanisms [2]. This interest has been boosted by the availability of radioactive-ion-beam facilities, which allowed experimental studies of reactions involving these nuclei [3–5]. One of their main features is the breakup process, which is supposed to be triggered by the Coulomb (nuclear) interaction when scattering on a heavy (light) target. The breakup process may affect other reaction channels such as fusion, and the assessment of this effect has been the subject of several theoretical and experimental efforts [6–31]. Nevertheless, this effect is still not totally clear and contradictory results coexist.

Experimentally, the breakup process can be studied by the detection in coincidence of all the breakup fragments [32–42]. In many cases, it requires neutron detection which can be rather involved from the experimental point of view. In addition, the breakup of light projectiles usually produces fragments with masses and charges similar to other light particles coming from different decay processes such as fusion, or even direct reaction channels such as transfers. For these reasons it is not easy to unambiguously identify the breakup process.

These studies are extremely difficult and time demanding to be performed with radioactive projectiles since they are produced as secondary beams with intensities several orders of magnitude lower than stable projectiles. Hence, stable weakly bound nuclei, such as ^{6}Li, ^{7}Li, and ^{9}Be, which are produced as primary beams with regular intensities, offer an excellent opportunity to perform systematic studies of angular distributions of their reaction products.

On the other hand, a big theoretical effort has been made over the last decades to develop coupled-channel calculation schemes to take into account the effect of the breakup process on the elastic-scattering angular distributions. Three-body and four-body continuum-discretized coupled-channel calculations have been applied to a number of cases with great success [31,43,44].

The nucleus of ^{9}Be presents a Borromean structure comprising two α particles and one neutron. Although stable, ^{9}Be has a small binding energy of 1.5736 MeV below the $\alpha + \alpha + n$ threshold [45]. Therefore, when colliding with a target nucleus, breakup effects are expected to be relevant. Experimental efforts have been made to better determine the ^{9}Be structure, such as works in Refs. [46–49]. Reactions induced by ^{9}Be have been already studied on ^{208}Pb at the Australian National University [50] and at the China Institute of Atomic Energy [51], on ^{27}Al at the University of São Paulo and on ^{27}Al and ^{144}Sm at the TANDAR Laboratory [24,52]. Regarding the target, the spherical (proton magic) ^{120}Sn nucleus has been investigated with weakly bound projectiles, both stable (^{6,7}Li [53]) and radioactive (^{6}He [43] and ^{8}Li [54]).

*arazi@tandar.cnea.gov.ar
†jcasal@us.es

The experimental data for elastic and breakup fragments produced in reactions involving these projectiles can be compared with continuum-discretized coupled-channel (CDCC) calculations [55,56], which include the coupling to the continuum part of the spectrum or breakup channels [30,57–59]. The CDCC formalism, first developed for two-body projectiles (three-body CDCC), was later extended to three-body projectiles (four-body CDCC) [57,58]. Very recently, the latter has been applied to ^{9}Be-induced reactions [60,61], taking into account its Borromean structure. In Ref. [61], the scattering of ^{9}Be on ^{208}Pb and ^{27}Al at energies around the Coulomb barrier was studied, showing that Coulomb breakup is still important at this energy range. The relevance of the ^{9}Be low-energy resonances on the angular cross sections was also shown.

To analyze the inelastic distributions due to the target excitation in the scattering of a weakly bound projectile, it would be desirable to include such excitations consistently within the CDCC formalism. Very recently, this extension has been addressed for the case of the three-body CDCC (i.e., for a two-body projectile) [62]. The feasibility of a similar approach for the four-body CDCC (three-body projectile) still needs to be studied. Nonetheless, coupled-channel (CC) calculations with collective form factors [63] can be performed by including explicitly the most important states and a bare potential to reproduce the interaction between projectile and target in the absence of coupling to the internal degrees of freedom.

In this work we present new measurements for the scattering of ^{9}Be on the intermediate-mass target ^{120}Sn carried out at the TANDAR Laboratory. In Sec. II, the experimental setup is addressed and the data is presented. In Sec. III, the measured elastic angular distributions are compared with an optical model (OM) analysis using the São Paulo potential (SPP) and with the four-body CDCC calculations. In Sec. IV, the experimental inelastic distributions are briefly analyzed with simple CC calculations. The summary and conclusions are given in Sec. V.

II. EXPERIMENTAL SETUP AND RESULTS

The experimental elastic- and inelastic-scattering angular distributions were obtained at the 20 UD tandem accelerator TANDAR at Buenos Aires. The ^{9}Be beams were mostly extracted as $^{9}BeO^{-}$ ions from the sputtering ion source, since their intensity (up to 1 μA at the ion source) is about 50 times higher than for atomic $^{9}Be^{-}$ ions. For the lower energies ($E_{lab} = 26, 27, 28, 29.5$, and 31 MeV), the 3+ charge state was selected, achieving a mean analyzed ^{9}Be intensity of 15 pnA. Since the accelerator was limited to a terminal voltage of 10 MV at the time of the experiment, the charge state 4+ was tuned for $E_{lab} = 42$ MeV, yielding 5 pnA. To achieve $E_{lab} = 50$ MeV, $^{9}Be^{-}$ ions were injected. In spite of their lower output at the ion source, $^{9}Be^{-}$ ions have a much better transmission at the stripper, since they do not suffer from the defocusing effect of the Coulomb explosion as the $^{9}BeO^{-}$ molecular beam. Besides, $^{9}Be^{-}$ ions have a higher yield for the $q = 4+$ charge state, achieving an analyzed intensity of 1 pnA.

Targets of enriched (>99%) ^{120}Sn, 85 μg/cm^2 thick, evaporated onto 20 μg/cm^2 carbon foils, were used at the center of a 70-cm-diameter scattering chamber. For some energies ($E_{lab} = 29.5$, 42, and 50 MeV), a stack of two targets was used to increase the counting rate. The energy loss in the target was calculated and the energy in its center was assumed as the reaction energy.

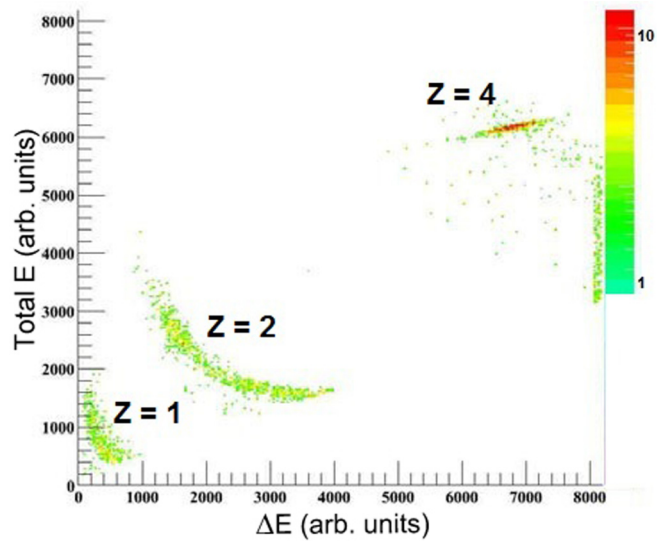

FIG. 1. Two-dimensional spectrum recorded at $\theta_{lab} = 170^{\circ}$ for $E_{lab} = 26$ MeV. The horizontal axis is the energy loss in the first stage of the telescope (ΔE) while the vertical one is the total energy obtained as $E = \Delta E + E_{res}$. The projection on this axis is equivalent to one-dimensional spectra obtained by single detectors. The $Z = 1$, $Z = 2$, and $Z = 4$ groups can be clearly identified.

An array of eight surface-barrier detectors (150 μm thick), with an angular separation of 5° between adjacent detectors, was used to distinguish scattering products. A liquid nitrogen cooling system set the detector temperature at −20 °C to improve their energy resolution, which varied between 0.5% and 1.0% (FWHM). This allowed us to separate two inelastic-excitation peaks with excitation energies of 1.19(5) and 2.41(5) MeV from the elastic-scattering peak.

The detectors were collimated by rectangular slits, defining an angular acceptance smaller than 0.5° and solid angles varying between 0.07 msr (most forward detector) and 0.8 msr (most backward detector). This assured comparable counting rates in all detectors. Additionally, a silicon telescope detector ΔE (15 μm) - E_{res} (150 μm) was placed at 170°. The E-ΔE two-dimensional spectra (see Fig. 1) allowed us to evaluate the composition of the background (mainly alpha particles arising from the projectile breakup) at angles at which the energy and counting rate of the elastic scattering are the lowest. It can be seen that alpha particles have lower energies than the elastically and inelastically scattered ^{9}Be and, therefore, they produced no interfering background, not even in the single detectors of our array, which only measure the total energy. Simulations performed with the code SUPERKIN [64], assuming the same relative energy for the breakup fragments as observed at 170°, allowed us to extend this result to forward angles.

A typical one-dimensional spectrum ($\theta_{lab} = 62.5^{\circ}$, $E_{lab} =$ 42 MeV) is shown in Fig. 2. For the peak integration, an asymmetric Gaussian curve was fit to the histograms with the

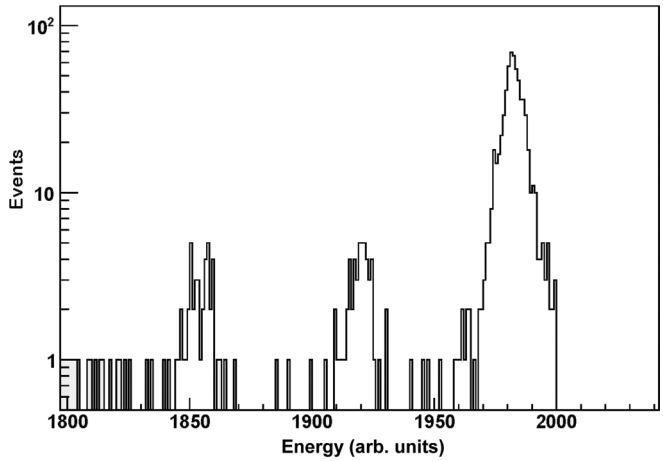

FIG. 2. Typical spectrum recorded at $\theta_{\rm lab} = 62.5^\circ$ for $E_{\rm lab} =$ 42 MeV. The large peak is due to the elastic scattering whereas the small peaks correspond to inelastic-scattering processes.

lower (upper) integration limit calculated as $x_{\rm low} = x_0 - 3\sigma_{\rm low}$ and $x_{\rm upp} = x_0 + 3\sigma_{\rm upp}$, where x_0 is the centroid and $\sigma_{\rm low}$ ($\sigma_{\rm upp}$) is the lower (upper) standard deviation.

The measured angular range extended from 22° to 170° (laboratory frame) except at the highest energies where the angular range was progressively reduced. For $E_{\rm lab} = 50$ MeV, the covered angular range was from 10° to 75°.

The normalization of cross sections was performed by using a monitor detector which remained at a fixed angle $\theta_{\rm mon} = 25^\circ$, where the scattering is pure Rutherford. The differential cross sections for the ith detector at angular position θ_i was then determined as

$$\frac{d\sigma}{d\Omega}(\theta_i) = \frac{d\sigma^{\rm Ruth}}{d\Omega}(\theta_{\rm mon})\frac{N_i}{N_{\rm mon}}\frac{J_i}{J_{\rm mon}}\frac{\Omega_{\rm mon}}{\Omega_i}, \qquad (1)$$

where N_i ($N_{\rm mon}$), J_i ($J_{\rm mon}$), and Ω_i ($\Omega_{\rm mon}$) are the number of events in the peak, the Jacobian for the laboratory to center-of-mass transformation and the solid angle of the ith detector (monitor), respectively. For determining the ratios between the solid angles of each detector and that of the monitor, several angular distributions were measured with the detector array placed at different angles (both forward and backward) for two systems at sub-Coulomb energies, ^{6}Li + ^{197}Au at $E_{\rm lab} = 19$ and 23 MeV and ^{16}O + ^{197}Au at $E_{\rm lab} =$ 58 MeV, for which the Rutherford angular distribution was assumed.

An independent normalization was given by a Faraday cup at the end of the beam line, far away from the target, which integrated the total charge delivered by the beam in each run.

The uncertainties in the cross-section values were estimated as the root of the sum of squares of (a) the statistical contribution from both detector and monitor counts, which was about 2% on average (7% maximal) for lower energies, except at the higher energies and backward angles, where it reached values of 20% or 30% due to the low counting, (b) differences between the cross-section values yielded by the normalization with the Faraday cup and with the monitor (less than 3% in most cases), and (c) 2% for other uncontrolled uncertainty sources as detector angular position (known better than 0.1°), beam deviation, peak integration, etc. Hence, the total uncertainties typically ranged from 3% to 8%, with the aforementioned exceptions.

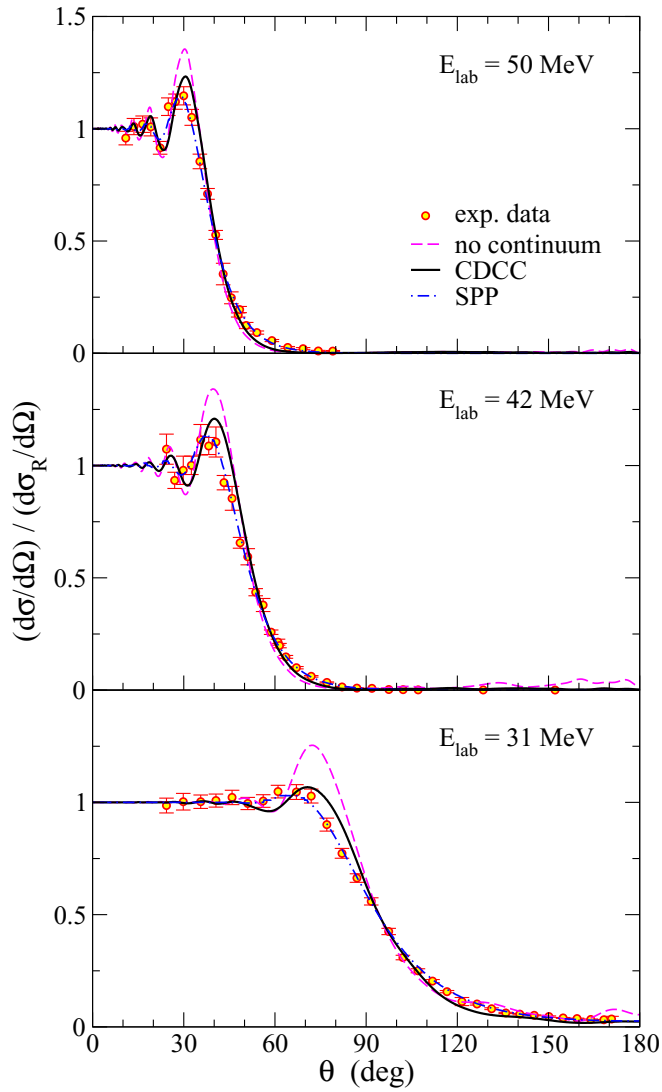

FIG. 3. Angular distribution of the elastic cross section relative to Rutherford for the reaction ^{9}Be + ^{120}Sn at $E_{\rm lab} = 50$, 42, and 31 MeV. The present experimental data are shown with circles. Dot-dashed lines correspond to optical model (OM) calculations using the São Paulo potential (SPP). Dashed lines correspond to four-body calculations including the ground state only, and solid lines show the full four-body CDCC calculations.

The experimental angular distributions of the elastic-scattering cross sections normalized to the Rutherford cross section are shown in Fig. 3 for the three highest energies measured ($E_{\rm lab} = 50$, 42, and 31 MeV), and in Fig. 4 for the other four energies ($E_{\rm lab} = 29.5$, 28, 27, and 26 MeV). The inelastic cross-section distributions are shown in Figs. 5 and 6 for the first and second peaks, respectively, at the three highest energies (50, 42, and 31 MeV).

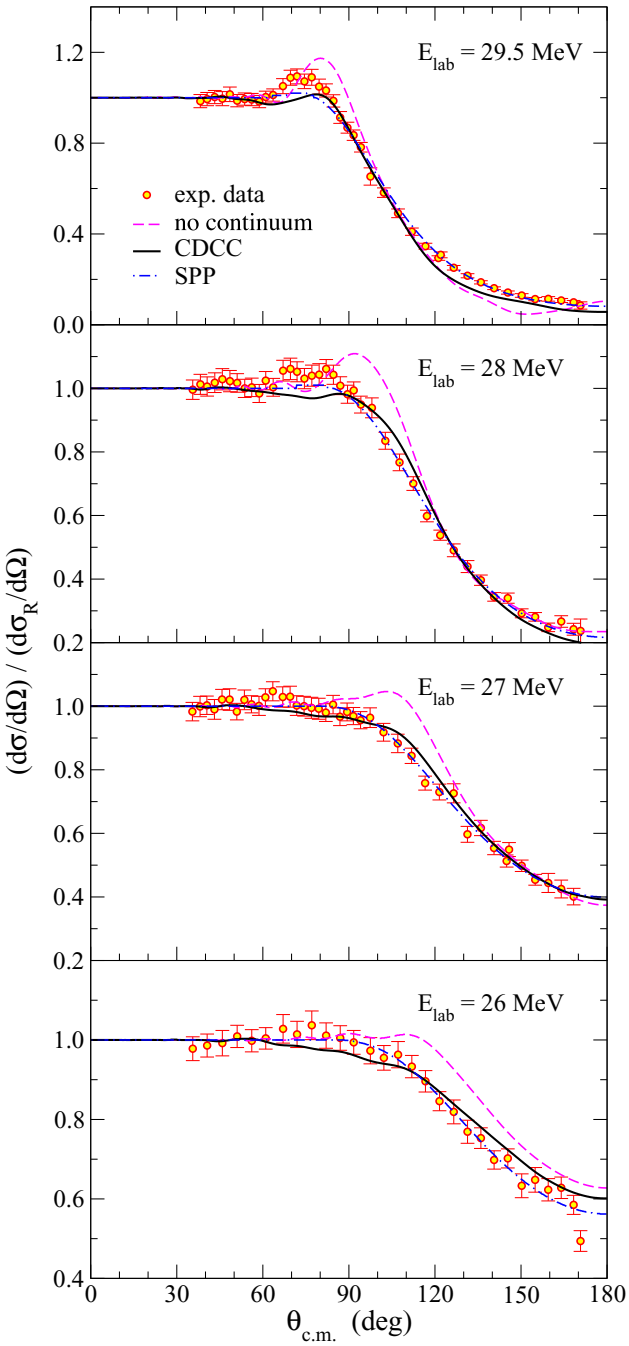

FIG. 4. Angular distribution of the elastic cross section relative to Rutherford for the reaction ^{9}Be + ^{120}Sn at $E_{\rm lab}$ = 29.5, 28, 27, and 26 MeV. The present experimental data are shown with circles. Dot-dashed lines correspond to optical model (OM) calculations using the São Paulo potential (SPP). Dashed lines correspond to four-body calculations including the ground state only, and solid lines show the full four-body CDCC calculations.

III. ANALYSIS OF ELASTIC SCATTERING

A. Optical model analysis

First, we performed optical model (OM) calculations using the São Paulo potential (SPP) [65,66]. In this model, the normalization factors of the real and the imaginary parts of the potential, N_r and N_i, respectively, are obtained by adjusting experimental elastic angular distributions at different bombarding energies. For the data of the present work, the best values obtained for these factors are presented in Table I. The quality of the fit is confirmed by the χ^2/ν values, which are close to unity. In Figs. 3 and 4 the OM fit for each energy is shown with a dot-dashed line and in Table II the calculated total reaction cross section for each energy is displayed.

In the case of tightly bound nuclei, the imaginary factor N_i drops at energies below the Coulomb barrier (with a corresponding peak in the real factor N_r); this effect is known as the threshold anomaly (TA). On the contrary, for some weakly bound nuclei N_i has been found to increase below the Coulomb barrier [8–10,67,68], which has been associated as the effect of the breakup channels still being open. This effect has been called the breakup threshold anomaly (BTA) [69].

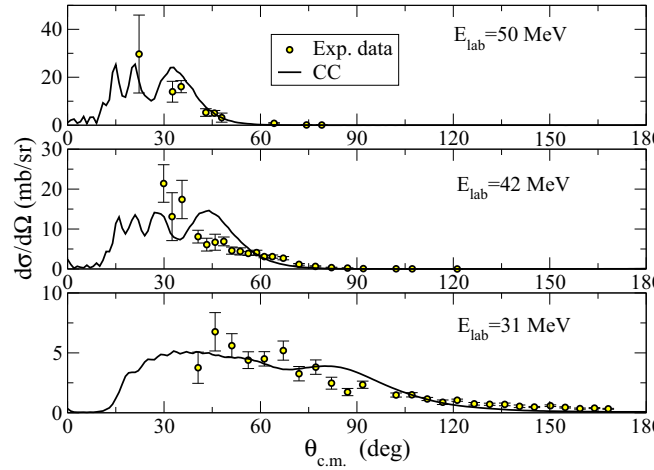

FIG. 5. Angular distribution of the inelastic cross section, considering an excitation of the ^{120}Sn to its 2_1^+ state, for the reaction ^{9}Be + ^{120}Sn at $E_{\rm lab}$ = 50, 42, and 31 MeV.

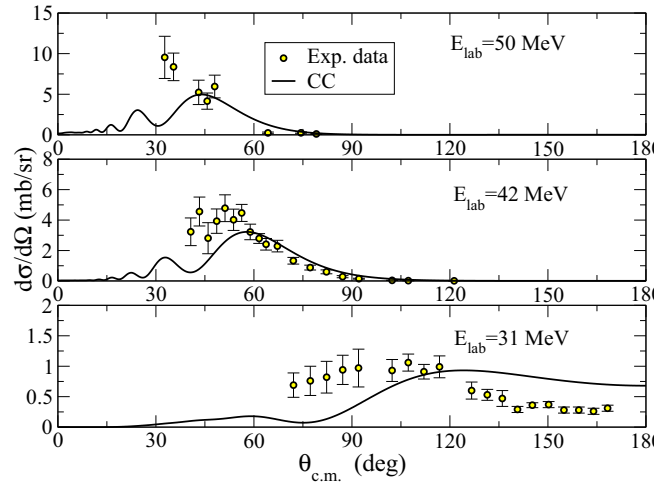

FIG. 6. Angular distribution of the inelastic cross section, considering an excitation of the ^{120}Sn to its 3_1^- state, for the reaction ^{9}Be + ^{120}Sn at $E_{\rm lab}$ = 50, 42, and 31 MeV.

TABLE I. Parameters of optical model calculations using the São Paulo potential: bombarding laboratory energy $E_{\rm lab}$, normalization factor for the real (imaginary) part N_r (N_i), number of measurements N, and reduced χ^2 value for fitting ($\nu = N - 2$ is the degree of freedom).

$E_{\rm lab}$ (MeV)	N_r	N_i	N	χ^2/ν
26	1.17(18)	1.24(15)	29	0.6
27	0.95(9)	1.29(9)	41	0.5
28	1.12(4)	1.12(6)	41	0.8
29.5	1.09(2)	1.18(5)	41	1.4
31	1.15(1)	1.39(5)	31	1.9
42	1.59(4)	1.57(9)	28	1.4
50	1.35(6)	1.66(15)	23	2.0

Intermediate cases in which neither behavior is clear have also been observed for ^{7}Li [10,67] and ^{9}Be [52] projectiles. For a global comparison using the same OM framework see Refs. [28,70,71].

Concerning ^{9}Be, there have been several OM calculations for different systems. The studies on the ^{9}Be + ^{209}Bi [51,72,73] and ^{9}Be + ^{208}Pb [51,73] systems suggest the presence of the BTA. However, for other targets such as ^{208}Pb [50], ^{27}Al [52], and ^{89}Y [74] the energy dependence does not present a clear trend.

Within the range of bombarding energies studied in the present work (see Fig. 7), the ^{9}Be + ^{120}Sn system shows a slight decreasing trend of the imaginary factor N_i at energies below the Coulomb barrier. However, this decrease is not as pronounced as in the usual threshold anomaly presented by tightly bound projectiles. This can be interpreted as absorptive channels still being open at energies below the nominal Coulomb barrier ($V_C \sim 28$ MeV). On the other hand, the expected breakup threshold anomaly (BTA), in which a rise of the imaginary term occurs before its final drop, is also not found. Thus, the behavior presented by the ^{9}Be + ^{120}Sn system seems to be closer to the anomaly presented by the weakly bound nucleus ^{7}Li [67,75].

B. Four-body continuum-discretized coupled-channel calculations

Loosely bound nuclei such as ^{9}Be are easily broken up into their constituents when colliding with another nucleus. This

TABLE II. Total reaction cross sections obtained from the OM analyses ($\sigma_R^{\rm OM}$) and from the four-body CDCC calculations ($\sigma_R^{\rm CDCC}$) for all the bombarding energies. Predictions for the total breakup cross sections ($\sigma_{\rm BU}^{\rm CDCC}$) are also given.

$E_{\rm lab}$ (MeV)	$\sigma_R^{\rm OM}$ (mb)	$\sigma_R^{\rm CDCC}$ (mb)	$\sigma_{\rm BU}^{\rm CDCC}$ (mb)
26	130	191	38.4
27	210	257	47.2
28	307	351	57.2
29.5	480	511	72.4
31	682	669	86.1
42	1610	1478	126.2
50	1980	1832	140.4

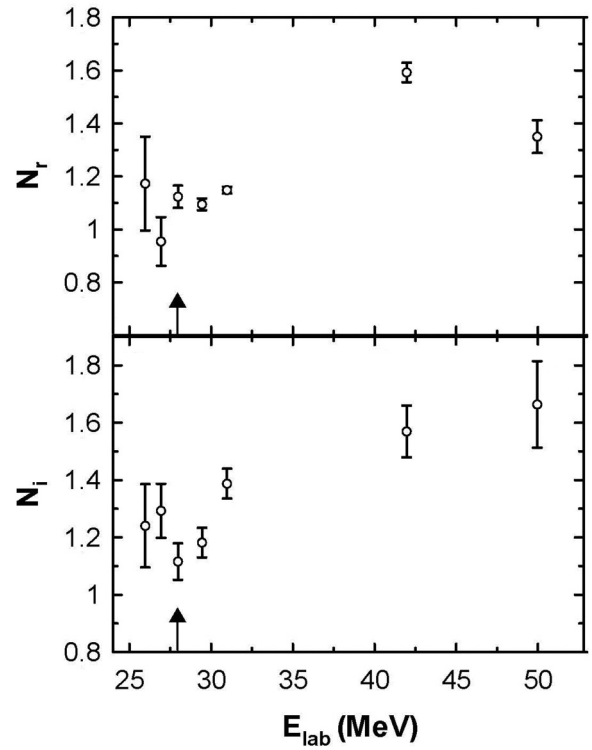

FIG. 7. Best real (N_r) and imaginary (N_i) normalization factors for the fitting of experimental elastic-scattering angular distributions of the ^{9}Be + ^{120}Sn system. The uncertainty bars are calculated according to the procedure of Ref. [70]. The vertical arrow shows the energy of the Coulomb barrier.

effect can be properly treated within the CDCC formalism [55,56], including the coupling to the continuum part of the spectrum. The scattering of ^{9}Be on ^{120}Sn can be described within the four-body CDCC framework considering the projectile, ^{9}Be, as a three-body system ($\alpha + \alpha + n$). The excitation of the target (as well as other possible channels such as core excitation or fusion) is included implicitly by the absorption due to the optical potentials between the projectile fragments and the target.

To describe the states of the projectile, we use the pseudostate method, which consists of diagonalizing the Hamiltonian in a discrete basis of square-integrable functions. Different bases have been used for three-body systems [57,60,76,77]. Here we use, as in Ref. [61], the analytical transformed harmonic-oscillator (THO) basis [78]. We refer the reader to Ref. [79] for details about the structure calculations for ^{9}Be using the analytical THO basis. Then, the ^{9}Be-^{120}Sn four-body wave functions are expanded in the internal states of the three-body projectile, leading to a coupled-equations system that has to be solved. For that, a multipole (Q) expansion is performed for each projectile fragment-target interacting potential. The procedure is explained in detail in Refs. [58,61].

The structure model for the three-body system ^{9}Be includes two-body potentials plus an effective three-body force. Since the three-body calculations are just an approximation to the full many-body problem, the parameters of the three-body potential are adjusted to reproduce the energy and matter

radius of the ground state ($j = 3/2^-$) and the energies of the known low-energy resonant states ($j = 1/2^+, 3/2^+, 1/2^-$, and $5/2^-$). The α-n potential is taken from Ref. [80] and the α-α potential is the Ali–Bodmer interaction [81], modified to reproduce the experimental phase shifts. These are shallow potentials in the sense that they include repulsive terms to remove unphysical two-body states. The parameters of the analytical THO basis chosen are those used also in Ref. [61]. The maximum hypermomentum is set to $K_{\max} = 10$ as in Ref. [61], which has been checked to provide converged results for reaction calculations at the range of energies considered. The convergence is also reached using a THO basis with $i_{\max} = 8$ hyper-radial excitations. The calculated ground-state energy is $\varepsilon_B = -1.574$ MeV and rms matter radius $r_{\text{mat}} = 2.466$ fm, to be compared with the experimental values $\varepsilon_B^{\text{expt}} = -1.5736$ MeV [45] and $r_{\text{mat}}^{\text{expt}} = 2.53$ fm [82].

The interactions between each projectile fragment and the target are represented by an optical potential, including both Coulomb and nuclear contributions. The n-^{120}Sn potential is represented by the Koning and Delaroche global parametrization [83] at the corresponding energy per nucleon. For the α-^{120}Sn interaction, we use the code by Kailas [84], which provides optical model parameters for α particles using the results from Ref. [85]. Our model space includes $j^\pi = 3/2^\pm$, $1/2^\pm$, and $5/2^\pm$ projectile states up to 8 MeV above the breakup threshold, which ensures convergence of the elastic angular distributions for this reaction. The coupled equations are solved up to $301/2$ partial waves, including continuum couplings to all multipole orders, i.e., up to $Q = 5$.

In Figs. 3 and 4 we show the four-body CDCC calculations at the different energies measured: 50, 42, 31, 29.5, 28, 27, and 26 MeV. Dashed lines are calculations including only the ground state of ^{9}Be and solid lines are the full CDCC calculations. In all cases, the agreement with the data is improved when we include the coupling to the continuum part of the spectrum. These couplings are important even at lower energies, where the inclusion of breakup channels is essential to describe the experimental cross sections. This result, together with Ref. [61], in which it is shown that the scattering on a light target at subbarrier energies exhibits a much smaller coupling to breakup channels, confirms that Coulomb breakup is an important process at low energies. This is a consequence of the weakly bound nature of ^{9}Be.

The agreement between the experimental data and the full four-body CDCC calculations is quite good overall. However, at energies of 29.5 and 28 MeV, the calculations underestimate the data in the nuclear-Coulomb interference region (between 60° and 90°, approximately). This effect has already been addressed for the reaction of ^{9}Be + ^{208}Pb [60,61], also at energies around the Coulomb barrier for this system. In principle, one expects that the scattering of a weakly bound nucleus such as ^{9}Be on a heavy target follows the same behavior reported, both experimentally and theoretically, for other weakly bound nuclei such as ^{6}He [43,86], ^{11}Li [29], ^{11}Be [87–89]. All these nuclei present a suppression of the rainbow at the interference region when colliding with heavy targets, as the energy decreases down to or below the Coulomb barrier. This is due to the strong dipolar Coulomb coupling to the continuum states, although nuclear coupling can be also important [88,90].

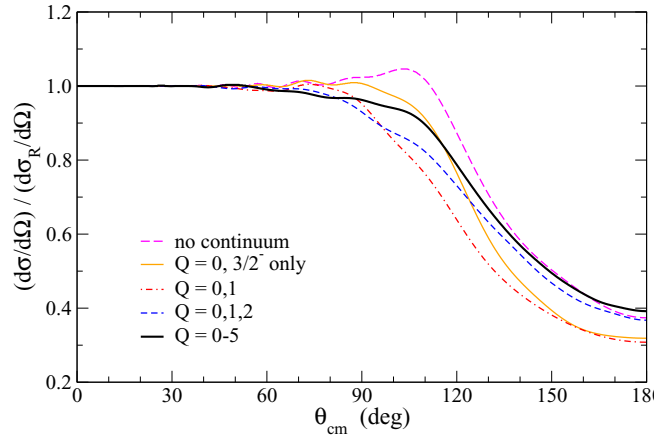

FIG. 8. Angular distribution of the elastic cross section relative to Rutherford for the reaction ^{9}Be + ^{120}Sn at $E_{\text{lab}} = 27$ MeV. The effect of the different j^π contribution and coupling multipolarities Q is shown.

Discrepancies in the nuclear-Coulomb interference region between the converged calculations and the experiment, in the present work and in Refs. [60,61], could be attributed either to unaccounted systematic errors in the experimental data or to the theoretical models used. Both model calculations [60,61] are consistent. A better understanding of this issue requires, in addition to the elastic data, breakup angular distributions. The comparison between the elastic and breakup channels at the same angular region could clarify the situation, and such an experiment is already being planned at the TANDAR Laboratory.

To study the effect of the j^π contributions and coupling multipolarities Q on the results, in Fig. 8 we show different calculations at $E_{\text{lab}} = 27$ MeV, i.e., around the Coulomb barrier. The monopolar ($Q = 0$) contribution allows us to connect the $3/2^-$ ground state to the $3/2^-$ continuum. Then, dipolar and higher-order terms introduce coupling between all j^π configurations considered.

We see in Fig. 8 that the main contributions to reduce the cross section, the monopole and dipole terms, are of the same order. A similar result has been reported previously for the scattering of ^{9}Be on ^{208}Pb [61]. This result differs from the case of the scattering of halo nuclei on heavy targets, e.g., ^{6}He or ^{11}Li on ^{208}Pb, where dipolar contributions produce the largest deviation with respect to the calculation without continuum couplings [29,58]. The ^{9}Be nucleus is a weakly bound system but presents a smaller $E1$ strength than typical halo nuclei [79]. This reduces the effect of dipolar couplings. Higher-order contributions also produce an important effect which improves the description of the experimental data in the whole angular region, but especially at backward angles.

Last, given that we have no experimental breakup data, we compare in Table II, the total reaction cross section for each energy as given for the four-body CDCC (σ_R^{CDCC}) calculations with the OM analyses (σ_R^{OM}). Both results are consistent considering that they come from very different approaches.

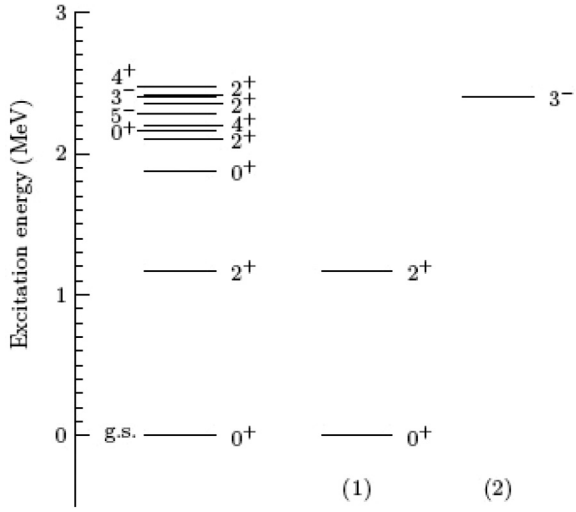

FIG. 9. Low-energy states of the ^{120}Sn nucleus. First column includes the known experimental levels. Second and third columns are the first states of the g.s. rotational band (1) and the negative-parity band (2), respectively.

Since the OM model is adjusted to the experimental data, this comparison supports the validity of the present CDCC calculations. These calculations also provide the total breakup cross sections ($\sigma_{\rm BU}^{\rm CDCC}$), which may serve as a prediction to guide future experiments on the breakup of ^{9}Be on ^{120}Sn.

IV. TARGET EXCITATION: INELASTIC DISTRIBUTIONS

As stated in Sec. II, the experimental setup allowed us to separate two inelastic peaks on the spectra, from the elastic-scattering peak, at the three highest incident energies ($E_{\rm lab}$ = 50, 42, and 31 MeV). These peaks correspond to excitation energies of 1.19(5) MeV and 2.41(5) MeV above the ground state (g.s.). The corresponding inelastic angular distributions are shown in Figs. 5 and 6, respectively.

Since ^{9}Be has no bound excited states, these peaks are attributed to excitations of the ^{120}Sn target nucleus. Looking at the ^{120}Sn known spectrum [91], the first-excited state appears at an energy of 1.171265(15) MeV, over the ground state (g.s., 0^+), with angular momentum 2^+. Above the first-excited state there are several states between 1.8 and 2.5 MeV (see Fig. 9). According to the energy for which the second inelastic peak is observed, the states that can contribute to this second peak are 3^- at 2.40030(5) MeV, 2^+ at 2.42090(3) MeV, 2^+ at 2.355383(24) MeV, and 4^+ at 2.465632(23) MeV. Clearly, the experimental energy resolution of the detectors (roughly about 200 keV) is not enough to distinguish individual contributions from these states to the second peak.

To study the target excitations in the reaction of ^{9}Be on ^{120}Sn, we need a structure model for ^{120}Sn. The nucleus of ^{120}Sn, and other even-even tin isotopes [92], do not exhibit neither typical rotational nor harmonic vibrational structure. The soft-rotator model [93,94] is usually used to describe the collective level structure of this kind of nuclei. In Ref. [92], this model is used to sort the low-energy ^{120}Sn states into, approximately, rotational bands. Following the referred work, the g.s. (0^+) and the first-excited state (2^+ at 1.17 MeV over the g.s.) are members of the so-called g.s. rotational band with $K \approx 0$ as bandhead. The 3^- state at 2.40 MeV is the first level of the $K \approx 0$ negative-parity band. The 2^+ at 2.36 MeV is the second state of the gamma band with $K \approx 0$ and was not included in the subsequent reaction calculation. Finally, the states 2^+ at 2.42 MeV and 4^+ at 2.47 MeV are not even included in the structure calculation. According to this, the first inelastic peak in the present work corresponds to the excitation to the first-excited state (2_1^+ at 1.17 MeV, g.s. band) and the second peak to the first octupole deformation state (3_1^- at 2.40 MeV). This assumption is also supported by the fact that 3_1^- is the only state, among the candidates, that has been detected by Coulomb excitation [91].

Here, to analyze the experimental inelastic distributions, we perform simple coupled-channels (CC) calculations with collective form factors [63], using matrix elements from a rigid rotor and taking the deformation parameters from the literature. The quadrupole and octupole deformation parameters associated with the excitation of the first 2^+ and 3^- states, respectively, are taken as $\beta_2 = 0.1075$ [95] and $\beta_3 = 0.1370$ [96]. From these values, the calculated deformation lengths are 0.6363 and 0.8109 fm, respectively. Apart from the deformation parameters, to perform the CC calculations is necessary to introduce a bare potential between the projectile and the target, i.e., the interaction between them in the absence of couplings to their internal degrees of freedom. For each energy, we use here, as bare potential, the optical potential obtained in Sec. III A for the OM analysis of the elastic data at such energy. The CC calculations were performed with the code FRESCO [97].

For the first-excited state, the CC calculations are shown in Fig. 5 with a full line. The comparison between experimental data and CC calculations is very good, confirming the excitation to the 2_1^+ state in ^{120}Sn. For the second peak, the agreement is not so good, especially at the most backward angles measured. In spite of the simplicity of the model calculation, these results indicate that the second peak must be due, at least mostly, to the excitation of the first octupole state 3_1^- at 2.40 MeV over the g.s.

V. SUMMARY AND CONCLUSIONS

We measured the elastic scattering of the ^{9}Be nucleus on a ^{120}Sn target at seven incident energies around and above the Coulomb barrier ($E_{\rm lab}$ = 50, 42, 31, 29.5, 28, 27, and 26 MeV) at the TANDAR laboratory. In addition, the energy resolution of cooled silicon detectors allowed us to separate two inelastic peaks on the spectra, from the elastic-scattering peak, at the three highest incident energies (50, 42, and 31 MeV) at excitation energies of 1.19(5) and 2.41(5) MeV.

The optical model analysis showed no significant drop of the absorption below the nominal Coulomb barrier, which can be interpreted as reaction channels being open for those energies. However, the appearance of a breakup threshold anomaly is not evident for this system.

The experimental elastic-scattering distributions have been compared with four-body CDCC calculations, describing the ^{9}Be projectile as a three-body system ($\alpha + \alpha + n$). The overall

agreement is quite good and the results show that the inclusion of the ^{9}Be continuum is relevant for the scattering process even at energies around and below the Coulomb barrier. This suggests that breakup is important even at low energies.

Simple CC calculations with collective form factors, using matrix elements from a rigid rotor, have been performed to confirm that the first inelastic peak measured corresponds to the excitation to the first-excited state of the ^{120}Sn nucleus, 2_1^+ at 1.17 MeV over the g.s. The calculations also suggest that the second inelastic peak likely corresponds to the octupole state 3_1^- at 2.40 MeV over the g.s.

ACKNOWLEDGMENTS

Authors are grateful to I. J. Thompson for his valuable support concerning technical details with the code FRESCO. This work has been partially supported by the Spanish Ministerio de Economía y Competitividad and the European Regional Development Fund (FEDER) under Projects No. FIS2014-51941-P and No. FIS2014-53448-c2-1-P, by Junta de Andalucía under Group No. FQM-160 and Project No. P11-FQM-7632 and by the European Union's Horizon 2020 research and innovation program under Grant Agreement No. 654002. J.C. acknowledges support from the Ministerio de Educación, Cultura y Deporte, FPU Research Grant No. AP2010-3124. M.R.-G. acknowledges postdoctoral support from theUniversidad de Sevilla under the V Plan Propio de Investigación Contract No. USE-11206-M. R.L. acknowledges Contract No. 2013/22100-7 from FAPESP (Brazil). The Argentinean authors acknowledge Grants No. PIP00786CO (CONICET) and No. PICT-2013-1363 (FONCyT).

[1] I. J. Thompson and F. M. Nunes, *Nuclear Reactions for Astrophysics* (Cambridge University Press, Cambridge, 2009).
[2] *Clusters in Nuclei*, edited by C. Beck (Springer-Verlag, Berlin, 2012), Vol. 2.
[3] Y. Blumenfeld, T. Nilsson, and P. V. Duppen, Phys. Scr. **152**, 014023 (2013).
[4] A. Lépine-Szily, R. Lichtenthäler, and V. Guimarães, Eur. Phys. J. A **50**, 128 (2014).
[5] R. Lichtenthäler *et al.*, Few-Body Syst. **57**, 157 (2016).
[6] D. J. Hinde, M. Dasgupta, B. R. Fulton, C. R. Morton, R. J. Wooliscroft, A. C. Berriman, and K. Hagino, Phys. Rev. Lett. **89**, 272701 (2002).
[7] A. Pakou, N. Alamanos, A. Gillibert, M. Kokkoris, S. Kossionides, A. Lagoyannis, N. G. Nicolis, C. Papachristodoulou, D. Patiris, D. Pierroutsakou, E. C. Pollacco, and K. Rusek, Phys. Rev. Lett. **90**, 202701 (2003).
[8] A. Pakou, N. Alamanos, A. Lagoyannis, A. Gillibert, E. Pollacco, P. Assimakopoulos, G. Doukelis, K. Ioannides, D. Karadimos, D. Karamanis, M. Kokkoris, E. Kossionides, N. Nicolis, C. Papachristodoulou, N. Patronis, G. Perdikakis, and D. Pierroutsakou, Phys. Lett. B **556**, 21 (2003).
[9] A. Pakou, N. Alamanos, G. Doukelis, A. Gillibert, G. Kalyva, M. Kokkoris, S. Kossionides, A. Lagoyannis, A. Musumarra, C. Papachristodoulou, N. Patronis, G. Perdikakis, D. Pierroutsakou, E. C. Pollacco, and K. Rusek, Phys. Rev. C **69**, 054602 (2004).
[10] J. M. Figueira, D. Abriola, J. O. Fernández Niello, A. Arazi, O. A. Capurro, E. de Barbará, G. V. Martí, D. Martínez Heimann, A. J. Pacheco, J. E. Testoni, I. Padrón, P. R. S. Gomes, and J. Lubian, Phys. Rev. C **73**, 054603 (2006).
[11] F. A. Souza, L. A. S. Leal, N. Carlin, M. G. Munhoz, R. Liguori Neto, M. M. de Moura, A. A. P. Suaide, E. M. Szanto, A. Szanto de Toledo, and J. Takahashi, Phys. Rev. C **75**, 044601 (2007).
[12] A. R. García, J. Lubian, I. Padron, P. R. S. Gomes, T. Lacerda, V. N. Garcia, A. G. Camacho, and E. F. Aguilera, Phys. Rev. C **76**, 067603 (2007).
[13] J. J. Kolata, H. Amro, F. D. Becchetti, J. A. Brown, P. A. DeYoung, M. Hencheck, J. D. Hinnefeld, G. F. Peaslee, A. L. Fritsch, C. Hall, U. Khadka, P. J. Mears, P. O'Rourke, D. Padilla, J. Rieth, T. Spencer, and T. Williams, Phys. Rev. C **75**, 031302 (2007).
[14] M. Sinha, H. Majumdar, R. Bhattacharya, P. Basu, S. Roy, M. Biswas, R. Palit, I. Mazumdar, P. K. Joshi, H. C. Jain, and S. Kailas, Phys. Rev. C **76**, 027603 (2007).
[15] C. Beck, N. Keeley, and A. Diaz-Torres, Phys. Rev. C **75**, 054605 (2007).
[16] M. Biswas, S. Roy, M. Sinha, M. K. Pradhan, A. Mukherjee, P. Basu, H. Majumdar, K. Ramachandran, and A. Shrivastava, Nucl. Phys. A **802**, 67 (2008).
[17] A. G. Camacho, P. R. S. Gomes, J. Lubian, and I. Padrón, Phys. Rev. C **77**, 054606 (2008).
[18] N. Keeley, K. W. Kemper, O. Momotyuk, and K. Rusek, Phys. Rev. C **77**, 057601 (2008).
[19] S. Mukherjee, B. K. Nayak, D. S. Monteiro, J. Lubian, P. R. S. Gomes, S. Appannababu, and R. K. Choudhury, Phys. Rev. C **80**, 014607 (2009).
[20] M. Y. M. Hassan, M. Y. H. Farag, E. H. Esmael, and H. M. Maridi, Phys. Rev. C **79**, 064608 (2009).
[21] Y. Kucuk, I. Boztosun, and N. Keeley, Phys. Rev. C **79**, 067601 (2009).
[22] D. S. Monteiro, O. A. Capurro, A. Arazi, J. O. Fernández Niello, J. M. Figueira, G. V. Martí, D. Martínez Heimann, A. E. Negri, A. J. Pacheco, V. Guimarães, D. R. Otomar, J. Lubian, and P. R. S. Gomes, Phys. Rev. C **79**, 014601 (2009).
[23] J. Lubian, T. Correa, E. F. Aguilera, L. F. Canto, A. Gomez-Camacho, E. M. Quiroz, and P. R. S. Gomes, Phys. Rev. C **79**, 064605 (2009).
[24] P. R. S. Gomes, J. Lubian, B. Paes, V. N. Garcia, D. Monteiro, I. Padrón, J. M. Figueira, A. Arazi, O. A. Capurro, L. Fimiani, A. E. Negri, G. V. Martí, J. O. Fernández Niello, A. Gómez-Camacho, and L. F. Canto, Nucl. Phys. A **828**, 233 (2009).
[25] L. F. Canto, P. R. S. Gomes, J. Lubian, L. C. Chamon, and E. Crema, Nucl. Phys. A **821**, 51 (2009).
[26] V. N. Garcia, J. Lubian, P. R. S. Gomes, A. Gomez-Camacho, and L. F. Canto, Phys. Rev. C **80**, 037602 (2009).
[27] F. A. Souza, C. Beck, N. Carlin, N. Keeley, R. L. Neto, M. M. de Moura, M. G. Munhoz, M. G. D. Santo, A. A. P. Suaide, E. M. Szanto, and A. S. de Toledo, Nucl. Phys. A **821**, 36 (2009).
[28] K. Zerva, A. Pakou, N. Patronis, P. Figuera, A. Musumarra, A. Di Pietro, M. Fisichella, T. Glodariu, M. La Commara, M. Lattuada, M. Mazzocco, M. G. Pellegriti, D. Pierroutsakou, A. M. Sanchez-Benitez, V. Scuderi, E. Strano, and K. Rusek, Eur. Phys. J. A **48**, 102 (2012).
[29] M. Cubero, J. P. Fernández-García, M. Rodríguez-Gallardo, L. Acosta, M. Alcorta, M. A. G. Alvarez, M. J. G. Borge, L. Buchmann, C. A. Diget, H. A. Falou, B. R. Fulton, H. O. U. Fynbo, D. Galaviz, J. Gómez-Camacho, R. Kanungo, J. A. Lay,

M. Madurga, I. Martel, A. M. Moro, I. Mukha, T. Nilsson, A. M. Sánchez-Benítez, A. Shotter, O. Tengblad, and P. Walden, Phys. Rev. Lett. **109**, 261701 (2012).
[30] J. P. Fernández-García, M. Cubero, M. Rodríguez-Gallardo, L. Acosta, M. Alcorta, M. A. G. Alvarez, M. J. G. Borge, L. Buchmann, C. A. Diget, H. A. Falou, B. R. Fulton, H. O. U. Fynbo, D. Galaviz, J. Gómez-Camacho, R. Kanungo, J. A. Lay, M. Madurga, I. Martel, A. M. Moro, I. Mukha, T. Nilsson, A. M. Sánchez-Benítez, A. Shotter, O. Tengblad, and P. Walden, Phys. Rev. Lett. **110**, 142701 (2013).
[31] V. Morcelle, K. C. C. Pires, M. Rodríguez-Gallardo, R. Lichtenthäler, A. Lépine-Szily, V. Guimarães, P. N. de Faria, D. R. M. Junior, A. M. Moro, L. R. Gasques, E. Leistenschneider, R. P. Condori, V. Scarduelli, M. Morais, A. Barioni, J. C. Zamora, and J. M. B. Shorto, Phys. Lett. B **732**, 228 (2014).
[32] A. C. Shotter, A. N. Bice, J. M. Wouters, W. D. Rae, and J. Cerny, Phys. Rev. Lett. **46**, 12 (1981).
[33] J. Hesselbarth and K. T. Knöpfle, Phys. Rev. Lett. **67**, 2773 (1991).
[34] V. Guimarães, J. J. Kolata, D. Peterson, P. Santi, R. H. White-Stevens, S. M. Vincent, F. D. Becchetti, M. Y. Lee, T. W. O'Donnell, D. A. Roberts, and J. A. Zimmerman, Phys. Rev. Lett. **84**, 1862 (2000).
[35] J. J. Kolata, V. Guimarães, D. Peterson, P. Santi, R. H. White-Stevens, S. M. Vincent, F. D. Becchetti, M. Y. Lee, T. W. O'Donnell, D. A. Roberts, and J. A. Zimmerman, Phys. Rev. C **63**, 024616 (2001).
[36] C. Signorini, A. Edifizi, M. Mazzocco, M. Lunardon, D. Fabris, A. Vitturi, P. Scopel, F. Soramel, L. Stroe, G. Prete, E. Fioretto, M. Cinausero, M. Trotta, A. Brondi, R. Moro, G. La Rana, E. Vardaci, A. Ordine, G. Inglima, M. La Commara, D. Pierroutsakou, M. Romoli, M. Sandoli, A. Diaz-Torres, I. J. Thompson, and Z. H. Liu, Phys. Rev. C **67**, 044607 (2003).
[37] A. Shrivastava, A. Navin, N. Keeley, K. Mahata, K. Ramachandran, V. Nanal, V. V. Parkar, A. Chatterjee, and S. Kailas, Phys. Lett. B **633**, 463 (2006).
[38] A. Pakou, N. Alamanos, N. M. Clarke, N. J. Davis, G. Doukelis, G. Kalyva, M. Kokkoris, A. Lagoyannis, T. Mertzimekis, A. Musumarra, N. Nicolis, C. Papachristodoulou, N. Patronis, G. Perdikakis, D. Pierroutsakou, D. Roubos, K. Rusek, S. Spyrou, and C. Zarkadas, Phys. Lett. B **633**, 691 (2006).
[39] A. Pakou, K. Rusek, N. Alamanos, X. Aslanoglou, S. Harissopulos, M. Kokkoris, A. Lagoyannis, T. J. Mertzimekis, A. Musumarra, N. G. Nicolis, C. Papachristodoulou, D. Pierroutsakou, and D. Roubos, Phys. Rev. C **76**, 054601 (2007).
[40] D. Martínez Heimann, A. J. Pacheco, O. A. Capurro, A. Arazi, C. Balpardo, M. A. Cardona, P. F. F. Carnelli, E. de Barbará, J. O. Fernández Niello, J. M. Figueira, D. Hojman, G. V. Marti, A. E. Negri, and D. Rodrigues, Phys. Rev. C **89**, 014615 (2014).
[41] S. Santra, V. V. Parkar, K. Ramachandran, U. K. Pal, A. Shrivastava, B. J. Roy, B. K. Nayak, A. Chatterjee, R. K. Choudhury, and S. Kailas, Phys. Lett. B **677**, 139 (2009).
[42] P. Carnelli, D. Martínez Heimann, A. J. Pacheco, A. Arazi, O. A. Capurro, J. O. Fernández Niello, M. A. Cardona, E. de Barbara, J. M. Figueira, D. L. Hojman, G. V. Marti, and A. E. Negri, Nucl. Phys. A **969**, 94 (2018).
[43] P. N. de Faria, R. Lichtenthäler, K. C. C. Pires, A. M. Moro, A. Lépine-Szily, V. Guimarães, D. R. J. Mendes, A. Arazi, M. Rodríguez-Gallardo, A. Barioni, V. Morcelle, M. C. Morais, O. Camargo, J. A. Nuñez, and M. Assunção, Phys. Rev. C **81**, 044605 (2010).
[44] K. C. C. Pires, R. Lichtenthäler, A. Lépine-Szily, V. Guimarães, P. N. de Faria, A. Barioni, D. R. Mendes Junior, V. Morcelle, R. P. Condori, M. C. Morais, J. C. Zamora, E. Crema, A. M. Moro, M. Rodríguez-Gallardo, M. Assunção, J. M. B. Shorto, and S. Mukherjee, Phys. Rev. C **83**, 064603 (2011).
[45] D. R. Tilley, J. H. Kelley, J. L. Godwin, D. J. Millener, J. E. Purcell, C. G. Sheu, and H. R. Weller, Nucl. Phys. A **745**, 155 (2004).
[46] B. R. Fulton, R. L. Cowin, R. J. Woolliscroft, N. M. Clarke, L. Donadille, M. Freer, P. J. Leask, S. M. Singer, M. P. Nicoli, B. Benoit, F. Hanappe, A. Ninane, N. A. Orr, J. Tillier, and L. Stuttge, Phys. Rev. C **70**, 047602 (2004).
[47] N. I. Ashwood, M. Freer, D. J. Millener, N. A. Orr, F. Carstoiu, S. Ahmed, J. C. Angelique, V. Bouchat, W. N. Catford, N. M. Clarke, N. Curtis, F. Hanappe, M. Horoi, Y. Kerckx, J. L. Lecouey, F. M. Marques, T. Materna, G. Normand, S. Pain, N. Soic, C. Timis, A. Unshakova, and V. A. Ziman, Phys. Rev. C **72**, 024314 (2005).
[48] P. Papka, T. A. D. Brown, B. R. Fulton, D. L. Watson, S. P. Fox, D. Groombridge, M. Freer, N. M. Clarke, N. I. Ashwood, N. Curtis, V. Ziman, P. McEwan, S. Ahmed, W. N. Catford, D. Mahboub, C. N. Timis, T. D. Baldwin, and D. C. Weisser, Phys. Rev. C **75**, 045803 (2007).
[49] T. Brown, P. Papka, B. Fulton, D. Watson, S. Fox, D. Groombridge, M. Freer, N. Clarke, N. Ashwood, N. Curtis, V. Ziman, P. McEwan, S. Ahmed, W. Catford, D. Mahboub, C. Timis, T. Baldwin, and D. Weisser, Phys. Rev. C **76**, 054605 (2007).
[50] R. J. Woolliscroft, B. R. Fulton, R. L. Cowin, M. Dasgupta, D. J. Hinde, C. R. Morton, and A. C. Berriman, Phys. Rev. C **69**, 044612 (2004).
[51] N. Yu, H. Q. Zhang, H. M. Jia, S. T. Zhang, M. Ruan, F. Yang, Z. D. Wu, X. X. Xu, and C. L. Bai, J. Phys. G **37**, 075108 (2010).
[52] P. R. S. Gomes, R. M. Anjos, C. Muri, J. Lubian, I. Padron, L. C. Chamon, R. L. Neto, N. Added, J. O. Fernández Niello, G. V. Marti, O. A. Capurro, A. J. Pacheco, J. E. Testoni, and D. Abriola, Phys. Rev. C **70**, 054605 (2004).
[53] D. Sousa *et al.*, Nucl. Phys. A **836**, 1 (2010).
[54] P. Neto de Faría, Ph.D. thesis, University of Sao Paulo, 2008.
[55] M. Yahiro, Y. Iseri, H. Kameyama, M. Kamimura, and M. Kawai, Prog. Theor. Phys. Suppl. **89**, 32 (1986).
[56] N. Austern, Y. Iseri, M. Kamimura, M. Kawai, G. Rawitsher, and M. Yahiro, Phys. Rep. **154**, 125 (1987).
[57] T. Matsumoto, T. Egami, K. Ogata, Y. Iseri, M. Kamimura, and M. Yahiro, Phys. Rev. C **73**, 051602(R) (2006).
[58] M. Rodríguez-Gallardo, J. M. Arias, J. Gómez-Camacho, R. C. Johnson, A. M. Moro, I. J. Thompson, and J. A. Tostevin, Phys. Rev. C **77**, 064609 (2008).
[59] J. A. Lay, A. M. Moro, J. M. Arias, and J. Gómez-Camacho, Phys. Rev. C **82**, 024605 (2010).
[60] P. Descouvemont, T. Druet, L. F. Canto, and M. S. Hussein, Phys. Rev. C **91**, 024606 (2015).
[61] J. Casal, M. Rodríguez-Gallardo, and J. M. Arias, Phys. Rev. C **92**, 054611 (2015).
[62] M. Gómez-Ramos and A. M. Moro, Phys. Rev. C **95**, 034609 (2017).
[63] T. Tamura, Rev. Mod. Phys. **37**, 679 (1965).
[64] D. Martínez Heimann, A. Pacheco, and O. Capurro, Nucl. Instrum. Methods Phys. Res., Sect. A **622**, 642 (2010).
[65] L. C. Chamon, D. Pereira, M. S. Hussein, M. A. C. Ribeiro, and D. Galetti, Phys. Rev. Lett. **79**, 5218 (1997).

[66] M. A. G. Alvarez, L. C. Chamon, M. S. Hussein, D. Pereira, L. Gasques, E. S. Rossi Jr., and C. Silva, Nucl. Phys. A **723**, 93 (2003).
[67] J. M. Figueira, J. O. Fernández Niello, A. Arazi, O. A. Capurro, P. Carnelli, L. Fimiani, G. V. Marti, D. Martínez Heimann, A. E. Negri, A. J. Pacheco, J. Lubian, D. S. Monteiro, and P. R. S. Gomes, Phys. Rev. C **81**, 024613 (2010).
[68] L. Fimiani, J. M. Figueira, G. V. Martí, J. E. Testoni, A. J. Pacheco, W. H. Z. Cárdenas, A. Arazi, O. A. Capurro, M. A. Cardona, P. Carnelli, E. de Barbará, D. Hojman, D. Martínez Heimann, and A. E. Negri, Phys. Rev. C **86**, 044607 (2012).
[69] M. S. Hussein, P. R. S. Gomes, J. Lubian, and L. C. Chamon, Phys. Rev. C **73**, 044610 (2006).
[70] D. Abriola, A. Arazi, J. Testoni, F. Gollan, and G. Marti, J. Phys.: Conf. Ser. **630**, 012021 (2015).
[71] D. Abriola, G. V. Marti, and J. E. Testoni, EPJ Web Conf. **146**, 02050 (2017).
[72] C. Signorini, A. Andrighetto, M. Ruan, J. Y. Guo, L. Stroe, F. Soramel, K. E. G. Lobner, L. Muller, D. Pierroutsakou, M. Romoli, K. Rudolph, I. J. Thompson, M. Trotta, A. Vitturi, R. Gernhauser, and A. Kastenmuller, Phys. Rev. C **61**, 061603 (2000).
[73] A. G. Camacho, N. Yu, H. Q. Zhang, P. R. S. Gomes, H. M. Jia, J. Lubian, and C. J. Lin, Phys. Rev. C **91**, 044610 (2015).
[74] C. Palshetkar, S. Santra, A. Shrivastava, A. Chatterjee, S. Pandit, K. Ramachandran, V. Parkar, V. Nanal, V. Jha, B. Roy, and S. Kalias, Phys. Rev. C **89**, 064610 (2014).
[75] J. M. Figueira, J. O. Fernández Niello, D. Abriola, A. Arazi, O. A. Capurro, E. deBarbara, G. V. Marti, D. Martínez Heimann, A. E. Negri, A. J. Pacheco, I. Padrón, P. R. S. Gomes, J. Lubian, T. Correa, and B. Paes, Phys. Rev. C **75**, 017602 (2007).
[76] I. J. Thompson, F. M. Nunes, and B. V. Danilin, Comput. Phys. Commun. **161**, 87 (2004).
[77] M. Rodríguez-Gallardo, J. M. Arias, J. Gómez-Camacho, A. M. Moro, I. J. Thompson, and J. A. Tostevin, Phys. Rev. C **72**, 024007 (2005).
[78] J. Casal, M. Rodríguez-Gallardo, and J. M. Arias, Phys. Rev. C **88**, 014327 (2013).
[79] J. Casal, M. Rodríguez-Gallardo, J. M. Arias, and I. J. Thompson, Phys. Rev. C **90**, 044304 (2014).
[80] I. J. Thompson, B. V. Danilin, V. D. Efros, J. S. Vaagen, J. M. Bang, and M. V. Zhukov, Phys. Rev. C **61**, 024318 (2000).
[81] S. Ali and A. R. Bodmer, Nucl. Phys. **80**, 99 (1966).
[82] E. Liatard *et al.*, Europhys. Lett. **13**, 401 (1990).
[83] A. J. Koning and J. P. Delaroche, Nucl. Phys. A **713**, 231 (2003).
[84] S. Kailas, Reference Input Parameter Library (RIPL-2), available online at http://www-nds.iaea.org/RIPL-2/.
[85] U. Atzrott, P. Mohr, H. Abele, C. Hillenmayer, and G. Staudt, Phys. Rev. C **53**, 1336 (1996).
[86] A. M. Sánchez-Benítez *et al.*, Nucl. Phys. A **803**, 30 (2008).
[87] A. Di Pietro, G. Randisi, V. Scuderi, L. Acosta, F. Amorini, M. J. G. Borge, P. Figuera, M. Fisichella, L. M. Fraile, J. Gomez-Camacho, H. Jeppesen, M. Lattuada, I. Martel, M. Milin, A. Musumarra, M. Papa, M. G. Pellegriti, F. Perez-Bernal, R. Raabe, F. Rizzo, D. Santonocito, G. Scalia, O. Tengblad, D. Torresi, A. M. Vidal, D. Voulot, F. Wenander, and M. Zadro, Phys. Rev. Lett. **105**, 022701 (2010).
[88] A. Di Pietro, V. Scuderi, A. M. Moro, L. Acosta, F. Amorini, M. J. G. Borge, P. Figuera, M. Fisichella, L. M. Fraile, J. Gomez-Camacho, H. Jeppesen, M. Lattuada, I. Martel, M. Milin, A. Musumarra, M. Papa, M. G. Pellegriti, F. Perez-Bernal, R. Raabe, G. Randisi, F. Rizzo, G. Scalia, O. Tengblad, D. Torresi, A. M. Vidal, D. Voulot, F. Wenander, and M. Zadro, Phys. Rev. C **85**, 054607 (2012).
[89] V. Pesudo, M. J. G. Borge, A. M. Moro, J. A. Lay, E. Nacher, J. Gomez-Camacho, O. Tengblad, L. Acosta, M. Alcorta, M. A. G. Alvarez, C. Andreoiu, P. C. Bender, R. Braid, M. Cubero, A. Di Pietro, J. P. Fernandez-Garcia, P. Figuera, M. Fisichella, B. R. Fulton, A. B. Garnsworthy, G. Hackman, U. Hager, O. S. Kirsebom, K. Kuhn, M. Lattuada, G. Marquinez-Duran, I. Martel, D. Miller, M. Moukaddam, P. D. OMalley, A. Perea, M. M. Rajabali, A. M. Sanchez-Benitez, F. Sarazin, V. Scuderi, C. E. Svensson, C. Unsworth, and Z. M. Wang, Phys. Rev. Lett. **118**, 152502 (2017).
[90] N. Keeley, N. Alamanos, K. W. Kemper, and K. Rusek, Phys. Rev. C **82**, 034606 (2010).
[91] K. Kitao, Y. Tendow, and A. Hashizume, Nucl. Data Sheets **96**, 241 (2002).
[92] J.-Y. Lee, I. Hahn, Y. Kim, S.-W. Hong, S. Chiba, and E. S. Soukhovitskii, Phys. Rev. C **79**, 064612 (2009).
[93] Y. V. Porodzinskij and E. S. Soukhovitskii, Phys. At. Nucl. **59**, 228 (1996).
[94] S. Chiba, O. Iwamoto, Y. Yamanouti, M. Sugimoto, M. Mizumoto, K. Hasegawa, E. S. Sukhovitskii, Y. V. Porodzinskii, and Y. Watanabe, Nucl. Phys. A **624**, 305 (1997).
[95] S. Raman, C. W. Nestor, and P. Tikkanen, At. Data Nucl. Data Tables **78**, 1 (2001).
[96] T. Kibedi and R. H. Spear, At. Data Nucl. Data Tables **80**, 35 (2002).
[97] I. J. Thompson, Comput. Phys. Rep. **7**, 167 (1988).